Behavioural Brain Research 405 (2021) 113188

Contents lists available at ScienceDirect

Behavioural Brain Research

journal homepage: www.elsevier.com/locate/bbr

Structural equation models to estimate dynamic effective connectivity networks in resting fMRI. A comparison between individuals with Down syndrome and controls

Maria Dolores Figueroa-Jiménez [a], Cristina Cañete-Massé [b,c], María Carbó-Carreté [d,e], Daniel Zarabozo-Hurtado [f], Joan Guàrdia-Olmos [b,c,e,*]

[a] Department of Health Sciences of the Centro Universitario de los Valles, University of Guadalajara, Mexico
[b] Department of Social Psychology & Quantitative Psychology Faculty of Psychology, University of Barcelona, Spain
[c] UB Institute of Complex Systems, University of Barcelona, Spain
[d] Serra Hunter Fellow, Department of Cognition, Developmental Psychology and Education, Faculty of Psychology, University of Barcelona, Spain
[e] Institute of Neuroscience, University of Barcelona, Spain
[f] RIO Group Clinical Laboratory, Center for Research in Advanced Functional Neuro-Diagnosis CINDFA, Guadalajara, Mexico

ARTICLE INFO

Keywords:
Dynamic functional connectivity
fMRI
Structural equation models
Down syndrome

ABSTRACT

Emerging evidence suggests that an effective or functional connectivity network does not use a static process over time but incorporates dynamic connectivity that shows changes in neuronal activity patterns. Using structural equation models (SEMs), we estimated a dynamic component of the effective network through the effects (recursive and nonrecursive) between regions of interest (ROIs), taking into account the lag 1 effect. The aim of the paper was to find the best structural equation model (SEM) to represent dynamic effective connectivity in people with Down syndrome (DS) in comparison with healthy controls. Twenty-two people with DS were registered in a functional magnetic resonance imaging (fMRI) resting-state paradigm for a period of six minutes. In addition, 22 controls, matched by age and sex, were analyzed with the same statistical approach. In both groups, we found the best global model, which included 6 ROIs within the default mode network (DMN). Connectivity patterns appeared to be different in both groups, and networks in people with DS showed more complexity and had more significant effects than networks in control participants. However, both groups had synchronous and dynamic effects associated with ROIs 3 and 4 related to the upper parietal areas in both brain hemispheres as axes of association and functional integration. It is evident that the correct classification of these groups, especially in cognitive competence, is a good initial step to propose a biomarker in network complexity studies.

1. Introduction

There are several options in regard to estimating connectivity networks from brain signal data. These options are available not only because there are different types of signals with varied information and behaviors but also because there are numerous techniques that allow, with more or fewer limitations, the identification of connectivity networks, whether they are functional or effective or whether they are static or dynamic. The study of brain function from the perspective of connectivity networks is a relatively recent approach and is an interesting option for investigating the concept of the brain as a complex system in which different parts of the brain interact under a certain pattern that must be identified. This type of connectivity pattern can be associated with different health states or cognitive characteristics that allow us to establish much more sensitive and precise brain complexity indicators than those used habitually in observational or psychometric records.

In relation to the different brain signals, the one that has been of most interest in the last ten years is the functional magnetic resonance imaging (fMRI) register. The reason for this preference may be because the fMRI signal allows for the generation of representational and mathematical models of brain function; also, although it is a somewhat cumbersome record, it is not as invasive to acquire fMRI data as it is to record other signals [1].

* Corresponding author at: Facultat de Psicología, Passeig de la Vall d'Hebrón, 171, 08035, Barcelona, Universitat de Barcelona, Spain.
E-mail address: jguardia@ub.edu (J. Guàrdia-Olmos).

https://doi.org/10.1016/j.bbr.2021.113188
Received 7 November 2020; Received in revised form 21 January 2021; Accepted 10 February 2021
Available online 23 February 2021

It seems clear and indisputable that since Biswal et al. [2] proposed the first works in a resting situation and estimated functional connectivity networks, we now have many options for application in this field. Lv et al. [3] offered a list of choices that adequately summarized the state-of-the-art options. A likely important point that the previous work likely highlights is, on one hand, the incorporation of dynamic connectivity network estimation in a resting situation and, on the other hand, the more current expert vision of systems estimation. In fact, the assumption that a static network obtained from BOLD signal behavior during an established period of time from *k* brain volumes is stable and unique is an assumption that is too banal and simple [4]. The idea of the existence of spatial property modifications of the network connection between brain areas (regions of interest, ROIs) is much closer to a structural and topological brain functioning concept. The effective or functional connectivity network presents a temporal evolution of its topological properties throughout the period of volume registration. This assumption, which brings us much closer to the conception of complex system models, must be taken into account to estimate much more realistic connectivity networks.

Certain aspects of dynamic connectivity have been studied in different populations, both in their functional and effective versions. It is true that most of the works have been proposed from the functional connectivity perspective and very few have been conducted involving effective dynamic connectivity. Some examples related to this are the work of Díez-Cirarda et al. [5], which showed differences in connectivity patterns between Parkinson's patients and a control group. Lin et al. [6] used dual signal pathway fMRI and EEG to study dynamic and static connectivity and to determine connectivity patterns in healthy control people. Chen et al. [7] went a step further and established the possibility that dynamic connectivity patterns could be considered a biomarker for discriminating between different levels of cognitive competence. Similar results were shown in the work of Threlkeld et al. [8], suggesting that consciousness recovery in patients with acute and severe traumatic brain injury (TBI) is associated with partial preservation of DMN correlations. Moreover, Ramani [9] showed that in patients with a genetic predisposition to Alzheimer's disease (AD), there is a connectivity alteration in the DMN from very early ages and before the appearance of any cognitive alteration.

There are a variety of options for solving this issue. The best-known model is the so-called dynamic causal model (DCM) described by Friston [10] and described by Park et al. [11] in a resting state situation. An excellent example of this approach can be found in Sharaev et al. [12] or Ye et al. [13]. The second option is the dynamic graphical model (DGM) defined by Schwab et al. [14], which proposes an algorithm for detecting a directed functional connectivity relationship between ROIs, using the mobile window technique to identify parent-child ROIs (according to the authors' terminology).

Nonetheless, an aspect that previous studies do not mention is the one linked to the use of structural equation models (SEMs) for the estimation of effective dynamic connectivity networks. There are multiple examples of the use of SEMs for effective static estimation that have been employed to establish the directionality of the relationships in the selected ROIs. Most of these contributions have been made, leaving aside the dynamic connectivity vision. For example, Guàrdia-Olmos et al. [15] showed effective connectivity networks in diabetic patients, and in the first meta-analysis, Guàrdia-Olmos et al. [16] showed the parameters estimated by an SEM in connectivity networks without dynamic components.

However, the idea of effective dynamic connectivity has still not been diligently explored, with even less work having been conducted in the field of SEMs. The recent appearance of the Group Iterative Multiple Model Estimation library (GIMME, 2020) opens an interesting option in the use of SEMs in effective dynamic connectivity [17,18]. The initial background on this issue can be identified as the one proposed by Zhang et al. [19] in the field of dynamic networks and language based on a previous mapping by Beltz & Gates [20]. However, the R library authors propose to understand dynamic network components from the estimable impact study of the number of short effects that are available to identify.

However, the concepts proposed by the authors of that library consist of understanding the dynamic component of the network from the study of the estimable impact of identifying the number of short effects, deemed lag 1 in the conception of the models. With this, it is possible to estimate the impact of an ROI at moment t on other ROIs at moment $t + 1$, which incorporates the dynamic effect in the estimation of the model. The effect of this concept is very limited, and the computational difficulties that SEM models have in this type of work must be taken into account. Inman et al. [21] argued these difficulties when highlighting the advantages of the GIMME option. The limitations of the GIMME option are also evident and focus on the impossibility of using a high number of ROIs as well as a short number of lag effects. Even so, the improvements are, in our opinion, evident.

From an application point of view, there are some works in dynamic connectivity that are important to mention. Pertinently, Chen et al. [7] with mild cognitive impairment (MCI) patients; Threlkeld et al. [8] with traumatic brain injury (TR) patients; Park et al. [11] showing a procedure for baseline estimation in dynamic connectivity studies; Sharaev et al. [12] with control subjects and study of small networks; Xu et al. [22] by studying the effect of methylphenidate in healthy subjects; Tang et al. [23] studying the effect of tobacco use in healthy subjects; Li et al. [24] with depressed patients; and finally, Xu et al. [25] studying dynamic connectivity in twins.

All the studies mentioned above and the knowledge about functional connectivity has become the basis of our work and can be summarized as follows: (a) there is evidence of a relationship between the topological properties of complex, basically functional brain networks and certain measures of cognitive performance [26–31]); (b) functional connectivity of the default mode network (DMN) is associated with the cognitive brain function [32–34]; (c) functional brain network connectivity is not a static process over time [35–47] (d) emerging evidence suggests that dynamic functional brain connectivity may indicate changes in the neuronal activity patterns that underlie critical aspects of cognition or clinically relevant information [38,40,46–50]; (e) dynamic connectivity is associated with the internal mental state both at rest and during the execution of a task [51]; and f) there is evidence of variability in dynamic functional connectivity networks. This variability is associated with the undirected tracking strategies that people often perform at rest [34]. Subregions of the DMN show decreasing variability activity when there is better resolution of cognitive tasks [52,53]. Thus, an increase in such undirected tracking would be linked to poorer task performance when responding to task stimuli, and it would be expected that this would translate into greater connectivity network complexity, whether dynamic or static.

The simplest comparison in cognitive terms lies in the analysis of the dynamic functional connectivity networks of healthy subjects in comparison with people with compromised cognitive functioning, for example, the Down syndrome (DS) population. These studies must strictly control the selection of the participants' age to avoid the presence of Alzheimer's disease (AD) or other cognitive diseases. The use of fMRI in individuals with DS has provided notable data that justify more in-depth studies of brain functioning in this population. Basically, previous works have shown that in people with DS, there is increased internetwork connectivity (i.e., hyperconnectivity) characterized by positive connectivity even in regions that are negative in control groups; as a consequence, there is a clear decreasing anti-correlation [54–56].

Taking the cited studies into consideration, the current work aimed to establish the dynamic effective connectivity networks of a DS group and another control, paired by age and sex, using SEMs. This was studied in a resting-state paradigm and only in part of the DMN (6 ROIs). It also aimed to determine if there is a different pattern between both groups and, finally, to assess the possibility of using those patterns to discriminate between groups.

Because of the results and the evidence of the abovementioned

works, we hypothesized that a) people with DS would show connectivity patterns at rest in a DMN network that would be much more complex than those that characterized in the control group and b) the SEM models for each group would show these effects, and it would be confirmed as a possible biomarker.

2. Material and method

2.1. Participants

The initial sample was composed of a total of 35 persons with DS (all participants had trisomy 21) between 16 and 35 years of age (M = 24.7 and SD = 5.49), and 26.5 % were women ($n_w = 9$). Accidental sampling was used, and recruitment took place through contact with different associations dedicated to DS in the state of Jalisco (México) (54.3 % of participants) and in Spain (45.7 %). The following inclusion and exclusion criteria were applied: a) age between 16 and 35 years and b) formal diagnosis of DS. The exclusion criteria were a) evidence of other comorbid diagnoses implying cognitive dysfunction (for example, the presence of dementia symptoms), b) inability to obtain consent from legal tutors, and c) the presence of medication affecting cognitive functions (specifically, for example, medication for mood regulation).

The intellectual disability diagnostic (out of 29 participants; the rest could not be accredited) revealed that 3.4 % had limited intellectual disability, 55.2 % had mild intellectual disability, 37.9 % had moderate intellectual disability and 3.4 % had profound intellectual disability. This classification appeared in the official report that each DS person presented at the time of incorporation into the study; limited intellectual disability is connected with the borderline zone, so this category does not appear in the ICD-10 categories (Codes F70-F79). A total of 84.4 % of the participants were right-handed, and 6.3 % of the participants were ambidextrous (n = 32). Laterality was directly assessed by a simple Praxis test during registration and confirmed with information from caregivers.

After recording the fMRI signal, data from ten of the 35 subjects were eliminated due to excessive movement during the recording, and some of them were even removed for the same reason after having repeated the recordings. Records with movement greater than ±2 degrees (or greater than half voxel size) were eliminated. Thus, the final sample for which fMRI was analyzed was composed of a total of 22 persons with DS, with the following observed age distribution: M = 25.55 and SD = 5.119. The distribution of the sample by sex indicated 22.7 % women. Whether any of the previous variables could be associated with failure to complete the fMRI record was analyzed. The relationship of the variables age, sex, and severity with whether the fMRI registry was completed was evaluated, and no statistically significant relationship was found.

A control group (n = 22) was included for comparison with the DS population. These subjects were obtained from the Human Connectome Project (http://www.humanconnectomeproject.org/), specifically from the open access dataset Autism Brain Imaging Data Exchange I (ABIDE I). ABIDE I is an image repository comprised of 17 international sites and collects structural and rest fMRI scans from people with autism spectrum disorder and healthy control groups. All data, including the phenotypic datasets and the protocol of acquisition parameters, are available at http://fcon_1000.projects.nitrc.org/indi/abide/abide_I. Only the control group of the ABIDE I dataset was used, and the subjects were selected to be matched with the DS sample by chronological age (M = 24,68; SD = 4.90; maximum 2-year difference in some subjects) and sex (22.7 % were women). No significant differences were found in relation to age (t = 0.568; df = 42; p = .573). To avoid any distortion in the image registry, only those registered in the control group with exactly the same technical characteristics as the registries used in the DS group were selected.

2.2. Instruments

The data from this work are part of a larger protocol in which the relationship between the brain signal (fMRI) and various variables connected with cognitive performance, quality of life and physical activity are being studied. In this case, only *ad hoc* questionnaires were used to assess the clinical and educational history, and the following variables were collected: age, sex, place of residence and degree of intellectual disability.

2.3. Procedure

Informed consent was obtained from each participant prior to the first neuropsychological screening session in accordance with the Declaration of Helsinki. Each of the three different protocols was approved by the Ethics Committee of the Bioethics Committee of the University of Barcelona. In accordance with this document, informed consent was obtained from the legal guardians of each person with DS and from the participants themselves. In addition, a medical report was obtained for each participant to rule out incompatibilities with image acquisition.

2.4. MRI image acquisition and preprocessing

After the administration of the scales, the participants underwent the fMRI recording sequence in the following order: T1-weighted, T2-weighted, FLAIR and 6-minute resting-state. Data were collected from March 2018 to July 2019. Two system models 3 T Philips Ingenia scanners (Phillips Healthcare) were used (one located at the Clinical Laboratory, Integral Medical Diagnostic Center of Guadalajara's RIO Group Center in Jalisco and the other at the Pasqual Maragall Foundation in Barcelona). A T1-weighted turbo field echo (TFE) structural image was obtained for each subject with a 3-dimensional protocol (repetition time [TR] =2300 ms, echo time [TE] =2980 ms, 240 slices, and field of view [FOV] = 240 × 240 × 170). Image acquisition was performed in the sagittal plane. For the functional images, a T2*-weighted (BOLD) image was obtained (TR =2000 ms, TE =30 ms, FOV = 230 × 230 × 160, voxel size = 3 × 3 × 3 mm, and slices = 29). Image acquisition was performed in the transverse plane. As previously mentioned, these technical characteristics correspond exactly to the records used in the control group.

During scanning, the participants were instructed to relax, remain awake, and keep their eyes open and fixed on a cross symbol on the screen. To avoid excessive movements, the necessary time was allocated for each person to get used to the registration situation. For this, the people who accompanied the members of the DS group were always visible, and during the habituation part of the session, they were able to be in the registration room. Obviously, at the beginning, there was no one in the registration room.

The structural imaging data were analyzed using an FSL (http://www.fmrib.ox.ac.uk/fsl/, RRID:SCR_002823) preprocessing pipeline adapted under authorization from Diez et al. [57], with its parameters adjusted to fit our experimental data, including a motion correction procedure to resolve the undesired head movements in the fMRI sessions.

In relation to fMRI data, the first 10 volumes were discarded for correction of the magnetic saturation effect, and the remaining volumes were slice-time corrected for temporal alignment. All voxels were spatially smoothed with a 6 mm FWHM isotropic Gaussian kernel, and after intensity normalization, a bandpass filter was applied between 0.01 and 0.08 Hz [58], which was followed by the removal of linear and quadratic trends. Finally, the functional data were spatially normalized to the MNI152 brain template.

T1-weighted images were reoriented to match the same axes as the templates, and a resampled AC-PC aligned image with six degrees of freedom (df) was created. All nonbrain tissue was removed to obtain an

anatomical brain mask that would be used to parcel and segment the T1-weighted image data. The use of DARTEL templates was ruled out since some previous analyses did not identify significant differences when using general templates. The final step involved registering our structural imaging data to normalized space using the Montreal Neurological Institute reference brain based on the Talairach and Tournoux coordinate system [59]. Finally, during the sessions, a caregiver of the person evaluated focused on helping the participants avoid unnecessary movements, aberrant behaviors or lack of adherence to the instructions that could lead to exclusion.

2.5. ROI's

The automated anatomical labeling (AAL) atlas [60] was used to define the ROIs. This atlas contains 45 cortical and subcortical areas in each hemisphere (90 areas in total), which are alternatively interspersed (available by request). To acquire the full signal of a given ROI, it was necessary to compute an average over the entire time series of all the voxels of a given brain area following the AAL atlas. In relation to the objective of the present study regarding the brain connectivity patterns in people with DS, we identified only the DMN. The posterior DMN subnetwork included the lateral parietal and middle temporal gyrus [61, 62], as indicated in Table 1. This selection was justified based on two criteria. The first criterion is that this network represents the most basic functioning of the DMN; therefore, it should be the most sensitive structure of all the subareas that comprise the most extensive DMN network (Farràs-Permanyer et al., 2019). The second criterion refers to the computational difficulties derived from estimating such a large number of possible structural models, which imposes a series of restrictions regarding the number of ROIs and networks to consider.

2.6. Statistical analysis

Once the images were preprocessed, correlation matrices were obtained between the 6 ROIs mentioned in Table 1 for each subject evaluated. To avoid the aberrant effect of values in some especially high or low ROIs (outliers), the jackknife correlation was estimated. There are other simulation possibilities for estimating statistical significance, but for small samples, jackknife correlation is still recommended. This technique consists of calculating all the correlation coefficients between all the possible ROI pairs, and one of the observations is excluded on each occasion. The average of all the correlations for each ROI pair attenuates the effects of the outliers. Each jackknife correlation coefficient was estimated using the following expression:

$$\theta_{(ROIi,ROIj)} = Jackknife\ Correlation\ Mean\ (ROIi, ROIj) = \frac{1}{n}\sum_{k=1}^{n} r_i$$

where r_i is Pearson's correlation between each pair of ROIs and n is the sample number in which the correlations in each pair have been estimated by extracting the record (volume) *i*. The SE of each average was also estimated from the expression:

$$SE = \sqrt{\frac{n-1}{n}\sum_{i=1}^{n}(r_i - \theta)^2}$$

This allowed confidence interval estimation for each correlation coefficient. Selecting either the correlation coefficient obtained with the whole sample or the one obtained through jackknife estimation depended on the bias value obtained. Bias was defined by the following expression:

$$Bias = (n-1) * (\theta - \hat{r})$$

For each correlation between ROIs, the bias value was obtained, and when it was close to 0, the average jackknife value was used. In cases in which bias was different from 0, the lower limit value of the confidence interval was used to avoid the probability of a type I error. To perform these analyses, the dist R library (3.6.3) was used. The different correlation matrices were used as input for the estimation of each SEM for each subject in both groups.

In essence, the adjustment of all structural models was performed by minimizing the matrix $(R - \Sigma)$. This expression involves the reproduction (Σ) of the initial matrix of correlations (R) between ROIs observed distributions. In other words, the result shows the best possible model for each subject, taking into account the incorporation of the recursive and nonrecursive effects between ROIs and incorporating the lag effects already described. A much broader description of SEMs applied to this context can be found in Guàrdia-Olmos et al. [16], and thus, under certain conditions, the SEM is exactly the same as the DCM. The difference in the current case, as already mentioned, is the incorporation of the dynamic effect.

3. Results

Table 2 shows the results of the adjustment models for each of the subjects analyzed according to the previously defined groups. It is important to highlight that this targeted classification offered a modularity value of 0.0139, which would indicate the nonexistence of other communities that were different from the two proposals, a group of DS persons and another group of control persons.

Tables 3a and 3b show the number of parameters with statistically significant effects in each of the six ROIs considered and differentiated for each group—persons with DS and controls. Fig. 1 summarizes these results and presents the total number of statistically significant parameters.

Table 1
Relationship of ROIs for the construction of the DMN according to the AAL90 atlas and their spatial localization.

DMN		
ROI	Roi AAL90	Region name
1	59	Parietal_Superior_Left
2	60	Parietal_Superior_Right
3	61	Parietal_Inferior_Left
4	62	Parietal_Inferior_Right
5	85	Temporal_Middle_Left
6	86	Temporal_Middle_Right

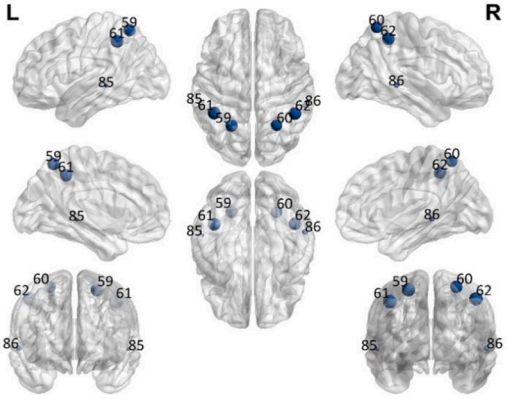

Table 2
Fit indexes of each SEM model.

SUBJ	χ^2	df	Ratio χ^2/df	Parameters estimated	p value	RMSEA	SRMR	NNFI	CFI	BIC	AIC	Log L	Group
1	191.8731	27	7.11	63	<.001	0.167	0.023	.910	.963	3414.03	3200.52	−1537.26	PWDS
2	218.4414	27	8.09	63	<.001	0.179	0.018	.899	.959	3274.80	3061.29	−1467.64	PWDS
3	241.6815	25	9.67	65	<.001	0.198	0.022	.897	.961	2376.82	2156.53	−1013.26	PWDS
4	168.9308	26	6.50	64	<.001	0.158	0.033	.919	.968	3377.41	3160.51	−1516.25	PWDS
5	225.2993	27	8.34	63	<.001	0.183	0.027	.884	.952	3763.02	3549.51	−1711.75	PWDS
6	227.5189	29	7.85	61	<.001	0.176	0.027	.922	.965	2058.62	1851.88	−864.94	PWDS
7	302.5942	28	10.81	62	<.001	0.211	0.036	.888	.952	2171.63	1961.51	−918.75	PWDS
8	218.4397	29	7.53	61	<.001	0.172	0.021	.922	.966	2365.59	2158.85	−1018.42	PWDS
9	231.1276	26	8.89	64	<.001	0.189	0.021	.889	.956	3263.38	3046.48	−1459.24	PWDS
10	338.1405	32	10.57	58	<.001	0.209	0.025	.873	.938	3036.03	2839.47	−1361.73	PWDS
11	174.5769	22	7.94	68	<.001	0.178	0.033	.909	.969	2857.04	2626.58	−1245.29	PWDS
12	340.9745	33	10.33	57	<.001	0.206	0.023	.903	.951	1651.15	1457.97	−671.98	PWDS
13	193.8546	31	6.25	59	<.001	0.154	0.030	.922	.963	3453.65	3253.70	−1567.85	PWDS
14	280.8342	31	9.06	59	<.001	0.191	0.019	.894	.950	2922.68	2722.73	−1302.36	PWDS
15	271.0832	30	9.04	60	<.001	0.191	0.034	.913	.960	1827.89	1624.55	−752.27	PWDS
16	299.5114	26	11.52	64	<.001	0.219	0.022	.892	.957	1589.88	1372.98	−622.49	PWDS
17	276.2692	32	8.63	58	<.001	0.186	0.016	.905	.954	2555.82	2359.26	−1121.63	PWDS
18	263.6547	28	9.42	62	<.001	0.196	0.021	.894	.955	2727.12	2517	−1196.5	PWDS
19	291.7739	25	11.67	65	<.001	0.220	0.017	.876	.953	2336.86	2116.57	−993.28	PWDS
20	275.042	35	0.79	55	<.001	0.177	0.036	.914	.954	2634.48	2448.08	−1169.04	PWDS
21	319.3598	37	8.63	53	<.001	0.186	0.024	.911	.950	2261.42	2081.80	−987.90	PWDS
22	417.0518	34	12.27	66	<.001	0.273	0.017	.796	.925	2847.41	2623.73	−1245.86	PWDS
23	197.524	28	0.71	62	<.001	0.166	0.044	.913	.963	3275.26	3065.14	−1470.57	Control
24	202.0626	32	6.31	58	<.001	0.155	0.024	.932	.967	2725.41	2528.84	−1206.42	Control
25	348.7178	36	9.69	54	<.001	0.199	0.024	.909	.950	1668.12	1485.11	−688.55	Control
26	209.3197	31	6.75	59	<.001	0.162	0.022	.905	.955	3883.22	3683.27	−1782.63	Control
27	334.9779	35	9.57	55	<.001	0.197	0.018	.906	.950	1986.09	1799.69	−844.84	Control
28	264.1082	36	7.34	54	<.001	0.170	0.014	.938	.966	1075.90	892.89	−392.44	Control
29	273.0015	35	7.80	55	<.001	0.176	0.036	.921	.958	2250.01	2063.61	−976.80	Control
30	232.3735	33	7.04	57	<.001	0.166	0.022	.922	.961	2763.95	2570.77	−1228.38	Control
31	192.4308	37	5.20	53	<.001	0.138	0.017	.940	.966	3204.28	3024.66	−1459.33	Control
32	254.8419	33	7.72	57	<.001	0.175	0.035	.928	.964	1754.87	1561.69	−723.84	Control
33	295.6647	35	8.45	55	<.001	0.184	0.018	.909	.952	2548.80	2362.41	−1126.20	Control
34	253.6002	35	7.25	55	<.001	0.168	0.022	.928	.962	2154.40	1968.00	−929.00	Control
35	263.7589	31	8.51	59	<.001	0.185	0.033	.921	.963	1679.04	1479.09	−680.54	Control
36	244.5833	39	6.27	51	<.001	0.155	0.014	.946	.968	1411.35	1238.51	−568.25	Control
37	322.3649	39	8.27	51	<.001	0.182	0.014	.916	.950	2215.97	2043.12	−970.56	Control
38	275.5027	35	7.87	55	<.001	0.177	0.017	.910	.952	2875.64	2689.24	−1289.62	Control
39	193.1305	31	6.23	59	<.001	0.154	0.028	.931	.968	2827.17	2627.21	−1254.60	Control
40	291.5398	39	7.48	51	<.001	0.172	0.027	.926	.956	2122.56	1949.71	−923.85	Control
41	307.095	31	0.99	59	<.001	0.201	0.028	.898	.952	2200.34	2000.38	−941.19	Control
42	291.1519	29	10.04	61	<.001	0.203	0.025	.889	.951	2597.86	2391.12	−1134.56	Control
43	334.1892	34	9.83	56	<.001	0.200	0.018	.905	.951	1843.28	1653.50	−770.75	Control
44	260.0007	39	6.67	51	<.001	0.160	0.049	.926	.956	2827.91	2655.07	−1276.53	Control

χ^2 = chi square estimation; df = degree of freedom; a ratio of χ^2/df > 3 indicates good fit; RMSEA = root mean square error adjusted (RMSEA ≈ 0 indicates a better fit); SRMR = standardized root mean residual (SRMR ≈ 0 indicates a better fit); NNFI = nonnormed fit index (NNFI > .90 indicates a better fit); CFI = comparative fit index (CIF > .90 indicates a better fit); BIC = Bayesian information criteria (smaller indicates a better fit); AIC = Akaike information criteria (smaller indicates a better fit); Log L = logarithm of maximum likelihood (ML) function (smaller indicates a better fit); PWDS = person with DS.

Table 3a
The number of statistically significant parameters in group number 1 of persons with DS.

	GROUP NUMBER 1											
	ROI1 Lag	ROI2 Lag	ROI3 Lag	ROI4 Lag	ROI5 Lag	ROI6 Lag	ROI1	ROI2	ROI3	ROI4	ROI5	ROI6
ROI1	22	0	22	3	2	5	0	0	22	3	2	6
ROI2	22	22	5	22	1	3	22	0	5	22	2	4
ROI3	2	3	22	22	7	1	2	2	0	22	7	2
ROI4	2	0	1	22	1	0	1	0	1	0	1	0
ROI5	1	6	6	1	22	22	4	5	6	2	0	22
ROI6	1	0	2	22	4	22	1	0	4	22	2	0

Given these results, concordances between the two groups were verified, especially regarding the variations in differential functioning of the effects related to ROI numbers 3 and 4 (Parietal_Left and Parietal_Lower_Right). Fig. 2 shows the characteristic SEM models of each group, taking into account the 22 subjects in each group at the same time.

Given these results, two subjects from each group with better-fitting SEMs were selected as examples. These four models are shown in Fig. 3.

Concerning the second proposed objective, the analysis described above was reproduced but without any directed classification. That is, we estimated the matrix of similarities among the 44 models to establish the number of detectable communities. The results showed a total of two communities, consistent with the number of groups defined (a control group and a DS group). Also, the modularity obtained in the nondirected classification was 0.0468, which would again indicate several communities no greater than those found.

Table 3b
The number of statistically significant parameters in the group of control persons.

	GROUP NUMBER 2											
	ROI1 Lag	ROI2 Lag	ROI3 Lag	ROI4 Lag	ROI5 Lag	ROI6 Lag	ROI1	ROI2	ROI3	ROI4	ROI5	ROI6
ROI1	22	2	2	1	2	2	0	1	2	1	3	2
ROI2	22	22	1	3	1	1	22	0	0	3	1	1
ROI3	2	1	22	22	3	2	3	3	0	22	4	2
ROI4	1	2	1	22	5	3	1	3	2	0	4	4
ROI5	0	1	2	1	22	22	0	1	1	2	0	22
ROI6	4	1	1	2	0	22	4	1	0	2	0	0

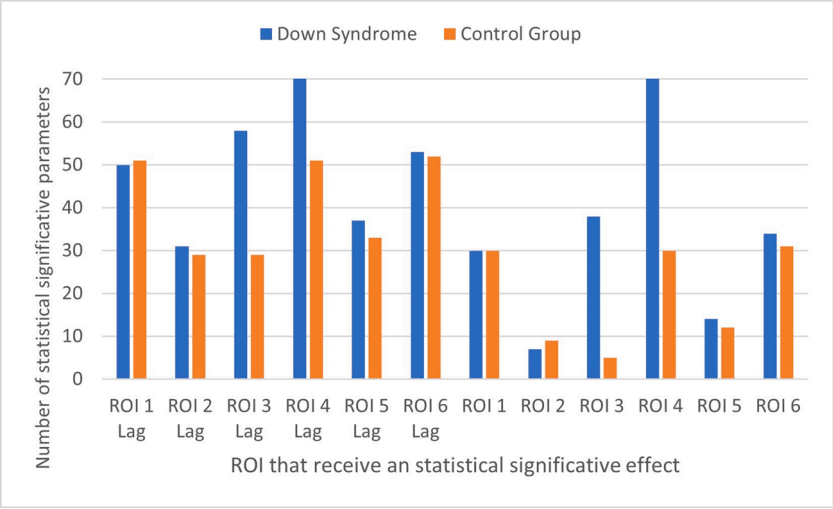

Fig. 1. The total number of statistically significant parameters detected in each of the two groups. Each column assumes the number of effects that each ROI receives, regardless of the original ROI, in a synchronous situation or lag 1.

These results imply that a total of 36 subjects (81.82 %) were correctly classified into two different groups: group number 1 consisting of individuals with DS (17) and group number 2 consisting of controls (19). In this case, the percentages of correct classification for each group were 77.27 % for the DS group and 86.36 % for the control group. However, 3 subjects in the control group were classified in the DS group, and 5 members in the DS group were classified in the control group. In addition, whether any of the sociodemographic variables could be related to the correct or incorrect classification was investigated. No statistically significant relationship was found that would allow us identify a systematic factor that would explain the correct or incorrect classification. Furthermore, it seems interesting that the percentage of correct classification was higher in the control group than in the DS group. We believe that the 9.09 % difference in correct classification between groups could be attributed to the fact that in the DS group, there is more intersubject variability that may make it difficult to recognize typical patterns for that group. However, the sample sizes do not allow for stronger explanations.

The differences in the SEM structure for each group can be complemented with the analysis of the statistically significant effect values found in each subject. Each of the 44 adjusted models was analyzed (Table 2) and the concrete values of the parameters between ROIs were studied; consequently, some evidence on the density of effects in each subject and group was obtained. For this purpose, all the values of the standardized parameters were positive, and the following results were obtained. In the group of DS persons, 251 significant effects were obtained, whereas in the group of control persons, only 98 were obtained, which implies an $OR = 2.56$. This clearly indicates a greater number of effects in the DS group. In relation to the value of the estimated parameters, in the DS group, the mean value was $M = 3.49$ ($SD = 0.293$), and in the control group, the mean value was $M = 4.21$ ($SD = 0.296$). The comparison between both means indicates a statistically significant effect [$t = 2.054$; $df = 347$; $p_{uni} = .0205$; 95 % *CI difference* = 1.41–3.05; $r = .11$], although with a smaller effect size. In relation to the characteristics of the effects, the values of the estimates were compared to evaluate synchronous effects and dynamic effects. The results indicated a total of 179 synchronous effects and 170 dynamic effects in lag 1. In this case, no statistically significant differences were found between these two types of effects in terms of parameter values (positivized) [$t = 0.972$; $df = 347$; $p = .332$]. In the case of synchronic effects, the average was $M = 3.54$ ($SD = 0.28$), and in the case of dynamic effects, $M = 3.85$ ($SD = 0.23$). Finally, the possible interaction between groups and types of effects was analyzed by simple factorial ANOVA. The results indicated that there was no statistically significant effect on the interaction between groups ($F = 0.045$; $df = 1, 345$; $p = .832$), so we must rule out differential effects between groups and effects. Therefore, between the two groups, differences were shown in the synchronous and dynamic effects associated with ROIs 3 and 4 and in the number of significant effects, which was greater in the case of the DS group, and that difference was not related to the synchronous or dynamic effects that were similar between the two groups. Finally, the parameter values in the control group were somewhat higher than those in the DS group, with a much lower number of significant effects but a somewhat higher value. Fig. 4 shows the most distinctive effects of all those shown in Fig. 2 but identifies the brain areas included in the dynamic effects. The effects that are more repeated in each group were selected to facilitate the identification of the best effects. Fig. 4 shows the most frequent effects in both groups.

4. Conclusions

In this paper, we compared the results obtained in the adjustment of

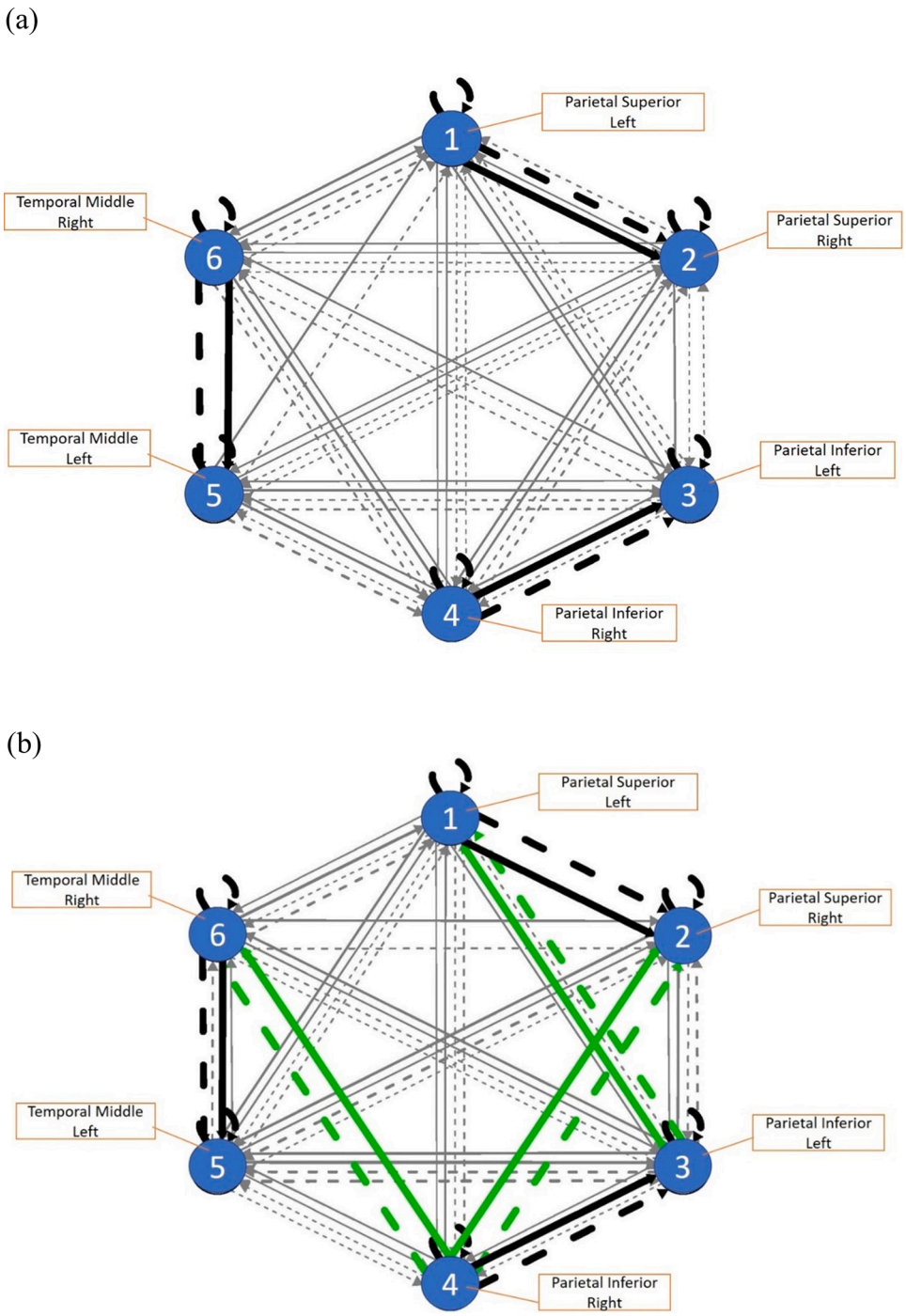

Fig. 2. Path diagram representation of each group. Black paths are at the group level, green paths are at the subgroup level, and gray paths are at the individual level; the thickness of the line represents the count.

dynamic SEMs (including the effects associated with lag 1) in two groups of people. One of them focused on DS persons, and the other focused on control persons. Both groups were paired by age and sex. The results were obtained with the GIMME library. Although the DS group showed more statistically significant effects (almost four times more effects of the control group), the impact effect was higher in the control group. There were no differences between the two groups concerning the number of synchronous or dynamic effects. Nevertheless, the structural differences between the global models of the two groups were associated with the presence of more effects between ROI numbers 3 and 4 in the DS group rather than the effects in the control group. These two ROIs imply the areas of the upper parts on the left and right, which indicates an asymmetrical effect in the synchronic estimation that is also manifested in the dynamic range defined in lag 1.

Buckner et al. [32]Bonnelle et al. [33] and Kucyi & Davis [34] found that DMN functional connectivity is associated with cognitive brain function. These areas integrate the association cortex related to the processing of all spatially oriented and fine motor stimuli that arrive through visual information. This connection is evident when we see that there are more effects between ROIs 3 and 4 in the DS group than in the control group. This is to be expected in task-involved studies such as in Garrett et al. [52] and Liang et al. [53]; these authors inferred that an increase in such undirected tracking would be linked to poorer task performance during task stimuli and that a greater complexity

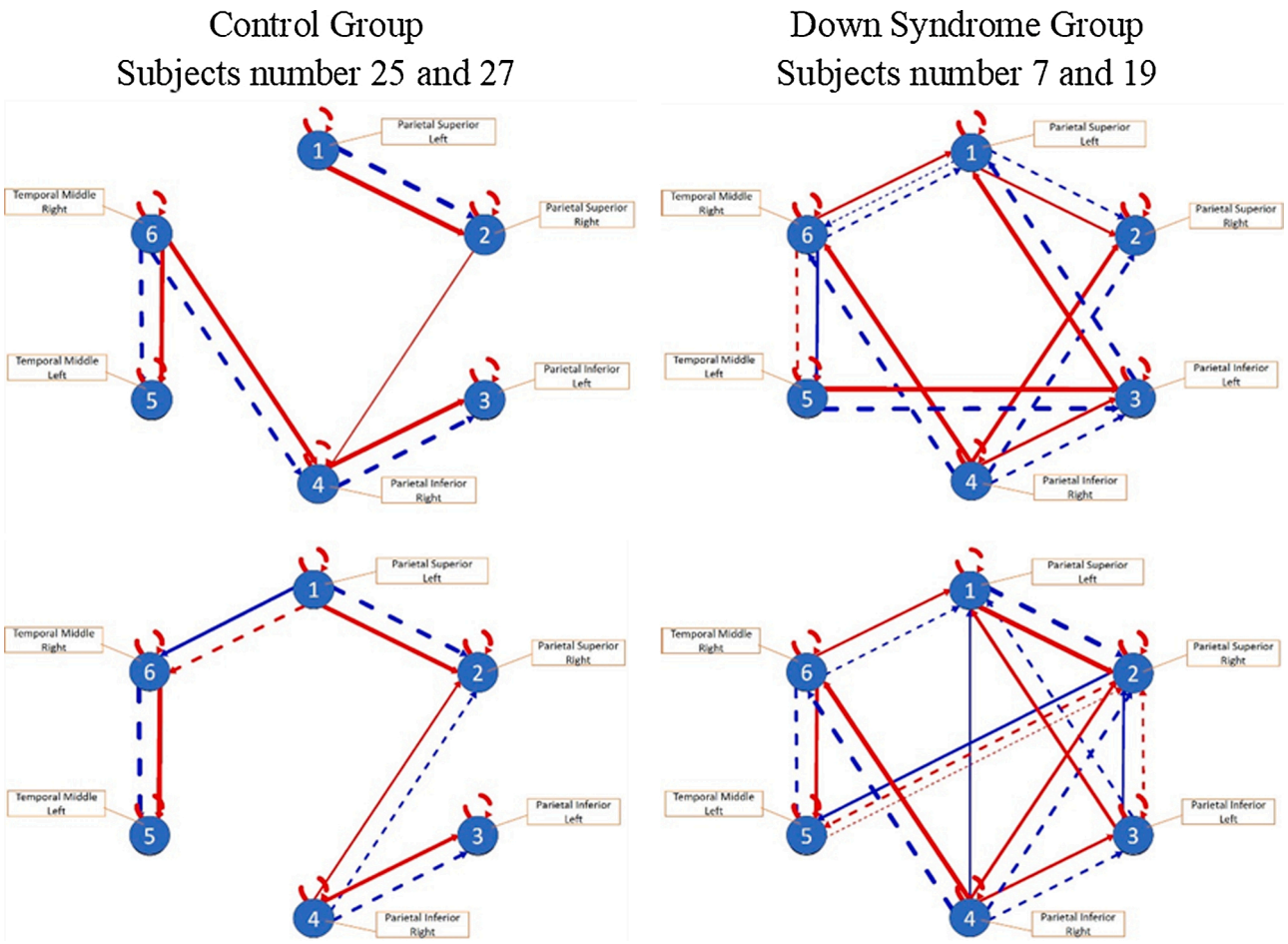

Fig. 3. Only two models from each group were selected to show the differences between adjusted SEMs. Red paths represent positive weights, and blue paths represent negative weights. Dashed lines denote lagged relations (lag 1), and solid lines are contemporaneous (lag 0).

connectivity network, whether dynamic or static, would be expected.

Through this study, we demonstrate that the same outcome is evident in a resting situation when comparing the DS group with a control group. This finding alludes that the connectivity patterns are different and that DS networks are more complex than control networks. Both of these characteristics are due to the existence of more significant effects in the DS group but with a lower value compared to that of the control group; the control group presents fewer effects but with a greater value than that of the DS group. Therefore, there is no difference concerning the synchronous effects following the dynamics. The difference between the DS group and the control group does not seem to be in the dynamic component; it seems to be more evident in the complexity component.

By taking into account the models of each person with DS and the control group using the SEM technique, we demonstrated that the network pattern could be a biomarker that clarifies and helps to discriminate the different levels of cognitive competence. In this case, the differences were very extreme given the conditions between both comparison groups. It is important to take into account that this study was conducted with two comparison groups with large differences between them. Therefore, it is important to initiate new studies with two groups that are not as different, mainly at the cognitive level. From our data, the very evident capacity to correctly distinguish between persons with DS and controls should be considered a good first step for the proposal of a biomarker based on the study of network complexity. The 81.82 % of correctly classified individuals found in our data is a good principle, but only that.

Furthermore, there was a sample percentage that was incorrectly classified (18.18 %), and we do not know what variables could explain this behavior. We should pay attention to these subjects in future studies to identify the cognitive properties and any other that could adequately describe the behavior of that blurred area between both groups.

The limitations we encountered were evident in the type of analysis that the SEM technique is based on. On the other hand, it is difficult to compare brain structures between persons with DS and controls, not only for morphological reasons but also for functioning. The sample size was small, and this must be taken into account in excessive generalizations. Moreover, the control group was not a group registered using the same protocol. It was a group extracted from the Connectome project and was a possible source of noise. In this sense, it seems reasonable to ask whether the use of a control group matched by mental age (not by chronological age) could offer interesting results in relation to the type of dynamic connectivity studied here. Our experience is that the generation of control groups matched by mental age implies, in general, such reduced mental ages that the comparison in neurofunctional and structural neural systems becomes difficult and is scarcely clarifying. However, this question should be addressed as soon as possible, and we expect to conduct a study between persons with DS and a control group matched by mental age that would confirm the results found here, since we understand that the question, in the case of people with DS, connectivity processes may be innately affected.

Similarly, the 6 ROIs evaluated showed limited connectivity and therefore had a very small scope. We must solve computer-related problems to carry out larger studies with complete brain atlases.

Apart from the above considerations, our data allowed us to identify the first results in the estimation of dynamic connectivity networks in a

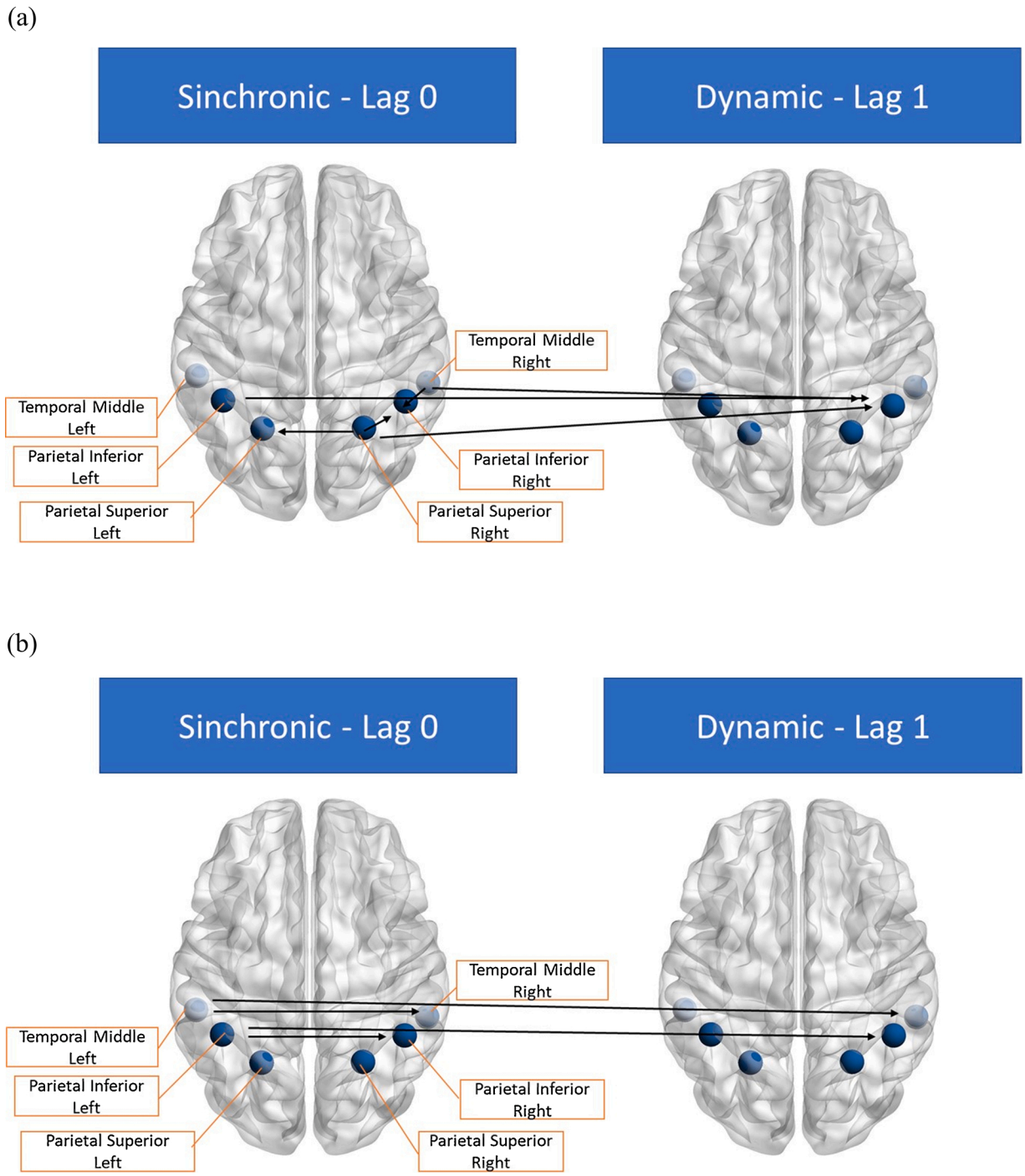

Fig. 4. Spatial representation of the global structural equation model for each group.

sample of DS people. Furthermore, there was enough evidence to affirm that there is a differential pattern of dynamic connectivity between a sample of DS people compared to a sample of controls, and that this pattern suggests that DS persons show a more complex connectivity network than that of the control group. These results, in addition, suggest that the complexity of a connectivity network could be an efficient biomarker for discrimination between these groups. Obviously, these statements should be reserved for the people evaluated, and studies with a greater number of ROIs are required, with a much more exhaustive analysis of the mediating variables that can occur in a complex population such as in people with DS (attention levels, mood, other comorbid structures, etc.). Finally, although the sample in this study was small, it was in line with other papers published with similar and even lower sample sizes.

Significance statement

This work shows, for the first time, that the structure of a dynamic connectivity network can discriminate between a group of people with compromised cognitive functions and a group of controls.

CRediT authorship contribution statement

Maria Dolores Figueroa-Jiménez: Conceptualization, Validation, Investigation, Writing - original draft, Writing - review & editing, Supervision. **Cristina Cañete-Massé:** Conceptualization, Methodology,

Software, Formal analysis, Investigation, Writing - original draft, Writing - review & editing, Supervision. **María Carbó-Carreté:** Conceptualization, Validation, Formal analysis, Investigation, Writing - original draft, Writing - review & editing, Supervision. **Daniel Zarabozo-Hurtado:** Conceptualization, Formal analysis, Investigation. **Joan Guàrdia-Olmos:** Conceptualization, Methodology, Software, Validation, Formal analysis, Resources, Data curation, Writing - original draft, Writing - review & editing, Visualization, Supervision, Funding acquisition.

Acknowledgements

The authors wish to thank all participants with Down syndrome, the participants' families and the participant's caregivers for their support and dedication to this research. We also thank the technologist and fMRI imaging specialists at the Rio Group Clinical Laboratory, Center for Research in Advanced Functional Neuro-Diagnostics CINDFA. Guadalajara (Mexico) and the Pascual Maragall Foundation for their help in acquiring the data reported in this article.

We thank the Ministry of Science, Innovation and Universities State Research Agency (Project code: PGC2018-095829-B-I00) for funding and support of this study.

The research sponsors were not involved in the design and conduct of the study; data collection, management, analysis, and interpretation; report writing and review; or the decision to submit the article for publication.

The manuscript describes independent research, and the opinions expressed are those of the authors.

References

[1] L.E. Mak, L. Minuzzi, G. MacQueen, G. Hall, S.H. Kennedy, R. Milev, The default mode network in healthy individuals: a systematic review and meta-analysis, Brain Connect. 7 (1) (2017) 25–33, https://doi.org/10.1089/brain.2016.0438.

[2] B. Biswal, F. Zerrin Yetkin, V.M. Haughton, J.S. Hyde, Functional connectivity in the motor cortex of resting human brain using echo-planar mri, Magn. Reson. Med. 34 (4) (1995) 537–541, https://doi.org/10.1002/mrm.1910340409.

[3] H. Lv, Z. Wang, E. Tong, L.M. Williams, G. Zaharchuk, M. Zeineh, A.N. Goldstein-Piekarski, T.M. Ball, C. Liao, M. Wintermark, Resting-state functional MRI: everything that nonexperts have always wanted to know, Am. J. Neuroradiol. 39 (8) (2018) 1390–1399, https://doi.org/10.3174/ajnr.A5527. PubMed.

[4] I. Cribben, Y. Yu, Estimating whole-brain dynamics by using spectral clustering, J. R. Stat. Soc. Ser. C Appl. Stat. 66 (3) (2017) 607–627, https://doi.org/10.1111/rssc.12169.

[5] M. Díez-Cirarda, A.P. Strafella, J. Kim, J. Peña, N. Ojeda, A. Cabrera-Zubizarreta, N. Ibarretxe-Bilbao, Dynamic functional connectivity in Parkinson's disease patients with mild cognitive impairment and normal cognition, Neuroimage Clin. 17 (2018) 847–855, https://doi.org/10.1016/j.nicl.2017.12.013.

[6] P. Lin, Y. Yang, J. Jovicich, N. De Pisapia, X. Wang, C.S. Zuo, J.J. Levitt, Static and dynamic posterior cingulate cortex nodal topology of default mode network predicts attention task performance, Brain Imaging Behav. 10 (1) (2016) 212–225, https://doi.org/10.1007/s11682-015-9384-6.

[7] H. Chen, F. Su, Q. Ye, Z. Wang, H. Shu, F. Bai, The dose-dependent effects of vascular risk factors on dynamic compensatory neural processes in mild cognitive impairment, Front. Aging Neurosci. 10 (2018) 131, https://doi.org/10.3389/fnagi.2018.00131.

[8] Z.D. Threlkeld, Y.G. Bodien, E.S. Rosenthal, J.T. Giacino, A. Nieto-Castanon, O. Wu, S. Whitfield-Gabrieli, B.L. Edlow, Functional networks reemerge during recovery of consciousness after acute severe traumatic brain injury, Cortex 106 (2018) 299–308, https://doi.org/10.1016/j.cortex.2018.05.004.

[9] R. Ramani, Connectivity, Curr. Opin. Anesthesiol. 28 (5) (2015). https://journals.lww.com/co-anesthesiology/Fulltext/2015/10000/Connectivity.4.aspx.

[10] K.J. Friston, Functional and effective connectivity: a review, Brain Connect. 1 (1) (2011) 13–36, https://doi.org/10.1089/brain.2011.0008.

[11] H.-J. Park, K.J. Friston, C. Pae, B. Park, A. Razi, Dynamic effective connectivity in resting state fMRI, NeuroImage 180 (2018) 594–608, https://doi.org/10.1016/j.neuroimage.2017.11.033.

[12] M.G. Sharaev, V.V. Zavyalova, V.L. Ushakov, S.I. Kartashov, B.M. Velichkovsky, Effective connectivity within the default mode network: dynamic causal modeling of resting-state fMRI data, Front. Hum. Neurosci. 10 (2016) 14, https://doi.org/10.3389/fnhum.2016.00014.

[13] A. Ye, K. Gates, T.R. Henry, L. Luo, Path and directionality discovery in individual dynamic models. A Regularized Unified Structural Equation Modeling Approach for Hybrid Vector Autoregression, 2020, https://doi.org/10.31219/osf.io/uh8ft.

[14] S. Schwab, R. Harbord, V. Zerbi, L. Elliott, S. Afyouni, J.Q. Smith, M.W. Woolrich, S.M. Smith, T.E. Nichols, Directed functional connectivity using dynamic graphical models, NeuroImage 175 (2018) 340–353, https://doi.org/10.1016/j.neuroimage.2018.03.074.

[15] J. Guàrdia-Olmos, E. Gudayol-Ferré, G.B. Gallardo-Moreno, M. Martínez-Ricart, M. Peró-Cebollero, A.A. González-Garrido, Complex systems representing effective connectivity in patients with type one diabetes mellitus, PLoS One 13 (11) (2018) 1–21, https://doi.org/10.1371/journal.pone.0208247.

[16] J. Guàrdia-Olmos, M. Peró-Cebollero, E. Gudayol-Ferré, Meta-analysis of the structural equation models' parameters for the estimation of brain connectivity with fMRI, Front. Behav. Neurosci. 12 (2018) 19, https://doi.org/10.3389/fnbeh.2018.00019.

[17] K.M. Gates, P.C.M. Molenaar, Group search algorithm recovers effective connectivity maps for individuals in homogeneous and heterogeneous samples, NeuroImage 63 (1) (2012) 310–319, https://doi.org/10.1016/j.neuroimage.2012.06.026.

[18] K.M. Gates, S.T. Lane, E. Varangis, K. Giovanello, K. Guskiewicz, Unsupervised classification during time-series model building, Multivariate Behav. Res. 52 (2) (2017) 129–148.

[19] X. Zhang, J. Yang, R. Wang, P. Li, A neuroimaging study of semantic representation in first and second languages, Lang. Cogn. Neurosci. (2020) 1–16, https://doi.org/10.1080/23273798.2020.1738509.

[20] A.M. Beltz, K.M. Gates, Network mapping with GIMME, Multivariate Behav. Res. 52 (6) (2017) 789–804, https://doi.org/10.1080/00273171.2017.1373014.

[21] C.S. Inman, G.A. James, S. Hamann, J.K. Rajendra, G. Pagnoni, A.J. Butler, Altered resting-state effective connectivity of fronto-parietal motor control systems on the primary motor network following stroke, NeuroImage 59 (1) (2012) 227–237, https://doi.org/10.1016/j.neuroimage.2011.07.083.

[22] F.F. Xu, L. Han, H.J. He, Y.H. Zhu, J.H. Zhong, Effective connectivity within the default mode network modulated by methylphenidate using dynamic causal modeling on resting-state functional magnetic resonance imaging, Acta Physiol. Sin. 68 (3) (2016) 255–264, https://doi.org/10.13294/j.aps.2016.0046.

[23] R. Tang, A. Razi, K.J. Friston, Y.-Y. Tang, Mapping smoking addiction using effective connectivity analysis, Front. Hum. Neurosci. 10 (2016) 195, https://doi.org/10.3389/fnhum.2016.00195.

[24] L. Li, B. Li, Y. Bai, W. Liu, H. Wang, H.-C. Leung, P. Tian, L. Zhang, F. Guo, L.-B. Cui, H. Yin, H. Lu, Q. Tan, Abnormal resting state effective connectivity within the default mode network in major depressive disorder: a spectral dynamic causal modeling study, Brain Behav. 7 (7) (2017) e00732, https://doi.org/10.1002/brb3.732.

[25] J. Xu, X. Yin, H. Ge, Y. Han, Z. Pang, B. Liu, S. Liu, K. Friston, Heritability of the effective connectivity in the resting-state default mode network, Cereb. Cortex 27 (12) (2017) 5626–5634, https://doi.org/10.1093/cercor/bhw332.

[26] N.U.F. Dosenbach, D.A. Fair, F.M. Miezin, A.L. Cohen, K.K. Wenger, R.A. T. Dosenbach, M.D. Fox, A.Z. Snyder, J.L. Vincent, M.E. Raichle, B.L. Schlaggar, S. E. Petersen, Distinct brain networks for adaptive and stable task control in humans, Proc. Natl. Acad. Sci. 104 (26) (2007) 11073–11078, https://doi.org/10.1073/pnas.0704320104.

[27] D.S. Bassett, E.T. Bullmore, A. Meyer-Lindenberg, J.A. Apud, D.R. Weinberger, R. Coppola, Cognitive fitness of cost-efficient brain functional networks, Proc. Natl. Acad. Sci. 106 (28) (2009) 11747–11752, https://doi.org/10.1073/pnas.0903641106.

[28] M.P. van den Heuvel, C.J. Stam, R.S. Kahn, H.E. Hulshoff Pol, Efficiency of functional brain networks and intellectual performance, J. Neurosci. 29 (23) (2009) 7619–7624, https://doi.org/10.1523/JNEUROSCI.1443-09.2009.

[29] P. Hagmann, O. Sporns, N. Madan, L. Cammoun, R. Pienaar, V.J. Wedeen, R. Meuli, J.-P. Thiran, P.E. Grant, White matter maturation reshapes structural connectivity in the late developing human brain, Proc. Natl. Acad. Sci. U. S. A. 107 (44) (2010) 19067–19072, https://doi.org/10.1073/pnas.1009073107. PubMed.

[30] N.A. Crossley, A. Mechelli, P.E. Vértes, T.T. Winton-Brown, A.X. Patel, C. E. Ginestet, P. McGuire, E.T. Bullmore, Cognitive relevance of the community structure of the human brain functional coactivation network, Proc. Natl. Acad. Sci. U. S. A. 110 (28) (2013) 11583–11588, https://doi.org/10.1073/pnas.1220826110. PubMed.

[31] P. Lin, J. Sun, G. Yu, Y. Wu, Y. Yang, M. Liang, X. Liu, Global and local brain network reorganization in attention-deficit/hyperactivity disorder, Brain Imaging Behav. 8 (4) (2014) 558–569, https://doi.org/10.1007/s11682-013-9279-3.

[32] R.L. Buckner, J.R. Andrews-Hanna, D.L. Schacter, The brain's default network, Ann. N. Y. Acad. Sci. 1124 (1) (2008) 1–38, https://doi.org/10.1196/annals.1440.011.

[33] V. Bonnelle, T.E. Ham, R. Leech, K.M. Kinnunen, M.A. Mehta, R.J. Greenwood, D. J. Sharp, Salience network integrity predicts default mode network function after traumatic brain injury, Proc. Natl. Acad. Sci. U. S. A. 109 (12) (2012) 4690–4695, https://doi.org/10.1073/pnas.1113455109. PubMed.

[34] A. Kucyi, K.D. Davis, Dynamic functional connectivity of the default mode network tracks daydreaming, NeuroImage 100 (2014) 471–480, https://doi.org/10.1016/j.neuroimage.2014.06.044.

[35] C. Chang, G.H. Glover, Time-frequency dynamics of resting-state brain connectivity measured with fMRI, NeuroImage 50 (1) (2010) 81–98, https://doi.org/10.1016/j.neuroimage.2009.12.011. PubMed.

[36] L. Cocchi, A. Zalesky, U. Toepel, T.J. Whitford, M. De-Lucia, M.M. Murray, O. Carter, Dynamic changes in brain functional connectivity during concurrent dual-task performance, PLoS One 6 (11) (2011), https://doi.org/10.1371/journal.pone.0028301 e28301-e28301. PubMed.

[37] D.A. Handwerker, V. Roopchansingh, J. Gonzalez-Castillo, P.A. Bandettini, Periodic changes in fMRI connectivity, NeuroImage 63 (3) (2012) 1712–1719, https://doi.org/10.1016/j.neuroimage.2012.06.078. PubMed.

[38] E. Tagliazucchi, F. von Wegner, A. Morzelewski, V. Brodbeck, H. Laufs, Dynamic BOLD functional connectivity in humans and its electrophysiological correlates, Front. Hum. Neurosci. 6 (2012), https://doi.org/10.3389/fnhum.2012.00339, 339-339. PubMed.
[39] J.-L. Chen, T. Ros, J.H. Gruzelier, Dynamic changes of ICA-derived EEG functional connectivity in the resting state, Hum. Brain Mapp. 34 (4) (2013) 852–868, https://doi.org/10.1002/hbm.21475. PubMed.
[40] R.M. Hutchison, T. Womelsdorf, E.A. Allen, P.A. Bandettini, V.D. Calhoun, M. Corbetta, S. Della Penna, J.H. Duyn, G.H. Glover, J. Gonzalez-Castillo, D. A. Handwerker, S. Keilholz, V. Kiviniemi, D.A. Leopold, F. de Pasquale, O. Sporns, M. Walter, C. Chang, Dynamic functional connectivity: promise, issues, and interpretations, NeuroImage 80 (2013) 360–378, https://doi.org/10.1016/j.neuroimage.2013.05.079. PubMed.
[41] R.M. Hutchison, T. Womelsdorf, J.S. Gati, S. Everling, R.S. Menon, Resting-state networks show dynamic functional connectivity in awake humans and anesthetized macaques, Hum. Brain Mapp. 34 (9) (2013) 2154–2177, https://doi.org/10.1002/hbm.22058. PubMed.
[42] A. Kucyi, T.V. Salomons, K.D. Davis, Mind wandering away from pain dynamically engages antinociceptive and default mode brain networks, Proc. Natl. Acad. Sci. 110 (46) (2013) 18692–18697, https://doi.org/10.1073/pnas.1312902110.
[43] H.-L. Lee, B. Zahneisen, T. Hugger, P. LeVan, J. Hennig, Tracking dynamic resting-state networks at higher frequencies using MR-encephalography, NeuroImage 65 (2013) 216–222, https://doi.org/10.1016/j.neuroimage.2012.10.015.
[44] N. Leonardi, J. Richiardi, M. Gschwind, S. Simioni, J.-M. Annoni, M. Schluep, P. Vuilleumier, D.V.D. Ville, Principal components of functional connectivity: a new approach to study dynamic brain connectivity during rest, NeuroImage 83 (2013) 937–950, https://doi.org/10.1016/j.neuroimage.2013.07.019.
[45] G.J. Thompson, M.D. Merritt, W.-J. Pan, M.E. Magnuson, J.K. Grooms, D. Jaeger, S. D. Keilholz, Neural correlates of time-varying functional connectivity in the rat, NeuroImage 83 (2013) 826–836, https://doi.org/10.1016/j.neuroimage.2013.07.036.
[46] E.A. Allen, E. Damaraju, S.M. Plis, E.B. Erhardt, T. Eichele, V.D. Calhoun, Tracking whole-brain connectivity dynamics in the resting state, Cereb. Cortex (New York, N.Y.: 1991) 24 (3) (2014) 663–676, https://doi.org/10.1093/cercor/bhs352. PubMed.
[47] E. Tagliazucchi, H. Laufs, Decoding wakefulness levels from typical fMRI resting-state data reveals reliable drifts between wakefulness and sleep, Neuron 82 (3) (2014) 695–708, https://doi.org/10.1016/j.neuron.2014.03.020.
[48] H.J. Park, K. Friston, Structural and functional brain networks: from connections to cognition, Science (New York, N.Y.) 342 (6158) (2013) 1238411, https://doi.org/10.1126/science.1238411.
[49] V.D. Calhoun, R. Miller, G. Pearlson, T. Adalı, The chronnectome: time-varying connectivity networks as the next frontier in fMRI data discovery, Neuron 84 (2) (2014) 262–274, https://doi.org/10.1016/j.neuron.2014.10.015.
[50] A. Kucyi, K.D. Davis, The dynamic pain connectome, Trends Neurosci. 38 (2) (2015) 86–95, https://doi.org/10.1016/j.tins.2014.11.006.
[51] A. Fornito, B.J. Harrison, A. Zalesky, J.S. Simons, Competitive and cooperative dynamics of large-scale brain functional networks supporting recollection, Proc. Natl. Acad. Sci. 109 (31) (2012) 12788–12793, https://doi.org/10.1073/pnas.1204185109.
[52] D.D. Garrett, N. Kovacevic, A.R. McIntosh, C.L. Grady, The importance of being variable, J. Neurosci. 31 (12) (2011) 4496, https://doi.org/10.1523/JNEUROSCI.5641-10.2011.
[53] X. Liang, Q. Zou, Y. He, Y. Yang, Coupling of functional connectivity and regional cerebral blood flow reveals a physiological basis for network hubs of the human brain, Proc. Natl. Acad. Sci. U. S. A. 110 (5) (2013) 1929–1934, https://doi.org/10.1073/pnas.1214900110. PubMed.
[54] J.S. Anderson, J.A. Nielsen, M.A. Ferguson, M.C. Burback, E.T. Cox, L. Dai, G. Gerig, J.O. Edgin, J.R. Korenberg, Abnormal brain synchrony in down syndrome, Neuroimage Clin. 2 (2013) 703–715, https://doi.org/10.1016/j.nicl.2013.05.006.
[55] J.N. Vega, T.J. Hohman, J.R. Pryweller, E.M. Dykens, T.A. Thornton-Wells, Resting-state functional connectivity in individuals with Down syndrome and Williams syndrome compared with typically developing controls, Brain Connect. 5 (2015) 461–475. https://10.1089/brain.2014.0266.
[56] L.R. Wilson, D. Vatansever, T. Annus, G.B. Williams, Y.T. Hong, T.D. Fryer, P. J. Nestor, A.J. Holland, S.H. Zaman, Differential effects of Down's syndrome and Alzheimer's neuropathology on default mode connectivity, Hum. Brain Mapp. 40 (2019) 4551–4563, https://doi.org/10.1002/hbm.24720.
[57] I. Diez, P. Bonifazi, I. Escudero, B. Mateos, M.A. Muñoz, S. Stramaglia, J.M. Cortes, A novel brain partition highlights the modular skeleton shared by structure and function, Sci. Rep. 5 (1) (2015) 10532, https://doi.org/10.1038/srep10532.
[58] D. Cordes, V.M. Haughton, K. Arfanakis, J.D. Carew, P.A. Turski, C.H. Moritz, M. A. Quigley, M.E. Meyerand, Frequencies contributing to functional connectivity in the cerebral cortex in "resting-state" data, Am. J. Neuroradiol. 22 (2001) 1326–1333.
[59] J. Ashburner, K.J. Friston, Nonlinear spatial normalization using basis functions, Hum. Brain Mapp. 7 (4) (1999) 254–266, https://doi.org/10.1002/(SICI)1097-0193(1999)7:4<254::AID-HBM4>3.0.CO;2-G.
[60] N. Tzourio-Mazoyer, B. Landeau, D. Papathanassiou, F. Crivello, O. Etard, N. Delcroix, B. Mazoyer, M. Joliot, Automated anatomical labeling of activations in SPM using a macroscopic anatomical parcellation of the MNI MRI single-subject brain, NeuroImage 15 (1) (2002) 273–289, https://doi.org/10.1006/nimg.2001.0978.
[61] L. Farras-Permanyer, N. Mancho-Fora, M. Montalà-Flaquer, D. Bartrés-Faz, L. Vaqué-Alcázar, M. Peró-Cebollero, J. Guàrdia-Olmos, Age-related changes in resting-state functional connectivity in older adults, Neural Regen. Res. 14 (9) (2019) 1544–1555, https://doi.org/10.4103/1673-5374.255976. PubMed.
[62] C.-C. Huang, W.-J. Hsieh, P.-L. Lee, L.-N. Peng, L.-K. Liu, W.-J. Lee, J.-K. Huang, L.-K. Chen, C.-P. Lin, Age-related changes in resting-state networks of a large sample size of healthy elderly, CNS Neurosci. Ther. 21 (10) (2015) 817–825, https://doi.org/10.1111/cns.12396.